


## Article

# Performance Analysis of Hybrid Desiccant Cooling System with Enhanced Dehumidification Capability Using TRNSYS

Ji Hyeok Kim <sup>1</sup> and Joon Ahn <sup>2,\*</sup> 

<sup>1</sup> Department of Mechanical Engineering, Graduate School, Kookmin University, Seoul 02707, Korea; wlgur0220@kookmin.ac.kr

<sup>2</sup> School of Mechanical Engineering, Kookmin University, Seoul 02707, Korea

\* Correspondence: jahn@kookmin.ac.kr; Tel.: +82-2-910-4833

**Abstract:** In a field test of a hybrid desiccant cooling system (HDCS) linked to a gas engine cogeneration system (the latter system is hereafter referred to as the combined heat and power (CHP) system), in the cooling operation mode, the exhaust heat remained and the latent heat removal was insufficient. In this study, the performance of an HDCS was simulated at a humidity ratio of 10 g/kg in conditioned spaces and for an increasing dehumidification capacity of the desiccant rotor. Simulation models of the HDCS linked to the CHP system were based on a transient system simulation tool (TRNSYS). Furthermore, TRNBuild (the TRNSYS Building Model) was used to simulate the three-dimensional structure of cooling spaces and solar lighting conditions. According to the simulation results, when the desiccant capacity increased, the thermal comfort conditions in all three conditioned spaces were sufficiently good. The higher the ambient temperature, the higher the evaporative cooling performance was. The variation in the regeneration heat with the outdoor conditions was the most dominant factor that determined the coefficient of performance (COP). Therefore, the COP was higher under high temperature and dry conditions, resulting in less regeneration heat being required. According to the prediction results, when the dehumidification capacity is sufficiently increased for using more exhaust heat, the overall efficiency of the CHP can be increased while ensuring suitable thermal comfort conditions in the cooling space.

**Keywords:** hybrid desiccant cooling system (HDCS); regeneration heat; cooling capacity; desiccant rotor; coefficient of performance (COP)



**Citation:** Kim, J.H.; Ahn, J. Performance Analysis of Hybrid Desiccant Cooling System with Enhanced Dehumidification Capability Using TRNSYS. *Appl. Sci.* **2021**, *11*, 3236. <https://doi.org/10.3390/app11073236>

Academic Editors: Xiaolin Wang and Paride Gullo

Received: 20 February 2021

Accepted: 27 March 2021

Published: 4 April 2021

**Publisher's Note:** MDPI stays neutral with regard to jurisdictional claims in published maps and institutional affiliations.



**Copyright:** © 2021 by the authors. Licensee MDPI, Basel, Switzerland. This article is an open access article distributed under the terms and conditions of the Creative Commons Attribution (CC BY) license (<https://creativecommons.org/licenses/by/4.0/>).

## 1. Introduction

Combined heat and power (CHP) systems recover exhaust heat from prime movers that generate electricity and use it for heating, which results in a high energy efficiency. However, because the power-to-heat ratio is fixed, energy load fluctuations during the different seasons and periods should be addressed to achieve high efficiency. In summer, when the heating system is not working, high efficiency can be achieved with a trigeneration system that includes a cooling system that uses exhaust heat [1]. Desiccant cooling systems, which are thermally driven cooling systems comprising combined cooling, heat, and power (CCHP) systems, are suitable for small-scale distributed energy systems (with electric power levels below 1 MW) [2].

Desiccant cooling systems supply hot dry air to the evaporative cooler. Instead of using electricity to compress the refrigerant, they use heat to regenerate the desiccant [3]. Desiccants can be classified into liquid and solid desiccants. The former are suitable for constructing high-capacity systems [3]. A system employing a solid desiccant can replace a household air-conditioner [4]. Solid desiccants are often manufactured in the form of wheels made of corrugated sheets [5].

For a solar-assisted desiccant cooling system with a solid desiccant, Seo et al. [6] analyzed the amount of sensible and latent heat during the months June, July, and August in Korea. Since the target temperature was set to be moderate (26 °C), sensible heat removal

was similar to latent heat removal [6]. Khalid et al. [7] studied a hybrid desiccant cooling system (HDCS) comprising three evaporative coolers and an auxiliary air-conditioner under Pakistani weather conditions. In their experiment, they found that the coefficient of performance increased slightly with ambient temperature. Moreover, they asserted that an HDCS assisted by solar thermal energy can achieve significant energy savings compared with the reheat vapor compression air-conditioning system [7]. Pi et al. [8] showed how the angular speed of a desiccant rotor affects the performance of the desiccant cooling system; the optimal rotation period of the desiccant rotor for the maximum dehumidification decreased when the humidity of the regeneration air decreased, regeneration temperature increased, and velocity of the process air decreased.

The cooling capacity of the desiccant cooling system is sensitive to outside air conditions. In humid climates, the cooling system is often equipped with a hybrid system connected to a heat pump [9]. Ahn et al. [10] experimentally investigated the performance characteristics of an HDCS for different outdoor conditions in a residential environment for two months. Its cooling capacity was found to be mainly affected by its latent heat removal ability and outdoor humidity [10].

Ahn and Choi [11] evaluated thermal comfort conditions when HDCSs were used in residential environments. Thermal comfort conditions can be assessed on the basis of various indicators [12]. Ahn and Choi [11] evaluated the ASHRAE comfort zone, predicted mean vote (PMV), and effective draft temperature (EDT). Conditioned spaces were included in the ASHRAE comfort zone under typical Korean summer outdoor conditions. However, both the PMV and EDT were not sufficiently good in certain locations, depending on the supply angle. In [10,11], an HDCS was used in apartment houses with district heating. In the current study, an HDCS was used in an office building and it was connected to a gas engine CHP system. When the HDCS was used, the indoor environment was outside the ASHRAE comfort zone under certain outdoor conditions. Kim and Ahn [13] analyzed the heat balance of a CHP system and discovered that there is room for exhaust heat in the cooling operation mode. The heat required to drive the HDCS in the present system was 14 kW, much less than 100 kW, which is the typical amount of heat recovered from a 100-kWe-class gas engine generator. Furthermore, in the current study, the performance resulting from an increase in the latent heat removal capacity was predicted on the basis of simulations by considering the cooling capacity of the HDCS to be sensitive to humidity [10].

For simulations, the transient system simulation tool (TRNSYS), which can include spatial and weather information of a conditioned space, was used. TRNSYS has been widely used to predict the performance characteristics of desiccant cooling systems. Jani et al. [14] simulated a solid-desiccant-assisted hybrid space cooling system by using TRNSYS. Caliskan et al. [15] used TRNSYS for thermodynamically assessing an HDCS, in which water for evaporative cooling was heated by solar thermal energy. Jani et al. [16] examined whether TRNSYS could be used to investigate the sustainability, feasibility, and potential use of desiccant-powered thermal space cooling systems. Finally, Sudhakar et al. [17] modeled a solar-assisted desiccant cooling system by using TRNSYS and MATLAB. An HDCS driven by a gas engine CHP system was installed in an office building at a university in Naju, Korea. Kim and Ahn [18] successfully predicted the transient behavior of temperature and humidity in an air-conditioned space through TRNSYS simulations.

In the current study, during the experiments in summer, the indoor thermal environment was out of the ASHRAE comfort zone under certain outdoor conditions, and consequently, additional temperature or humidity control was required to meet the comfort zone conditions. The dehumidification capacity was increased since there was room for exhaust heat generated by the CHP [13]. The target humidity ratio of the indoor space was maintained at 10 g/kg, which is representative of the ASHRAE comfort zone. A series of TRNSYS simulations for 39 outdoor condition scenarios with increased desiccant capacity for humidity control was performed.

In the CCHP system, if the heat used for cooling is less than that used for heating, there is scope for additional desiccant regeneration. For the effective use of this information for a hybrid system, a performance analysis based on the contributions of desiccant cooling and the heat pump should be performed. To date, many studies have been conducted on hybrid desiccant cooling, but there has been no study on the performance change when the desiccant regeneration capacity is increased. In this study, a CHP system and a TRNSYS model were developed, and simulated thermal indoor conditions were validated with experimental results. Subsequently, the change in the thermal comfort conditions resulting from an increase in the desiccant capacity was predicted. Performance data for different outside air conditions obtained from simulations were compared with the data of Ahn et al. [10] to investigate the performance change of the HDCS resulting from an increase in the desiccant capacity.

## 2. CCHP System

### 2.1. Configuration of Heat Recovery System

A schematic of the CCHP system investigated in this study is shown in Figure 1. By using natural gas as fuel, the gas engine produces electricity and recovers heat from the coolant jacket water and exhaust gas. The heat recovered by the heat recovery coolant is transferred to the heat storage tank and stored in the form of hot water. The hot water is supplied to the HDCS and used to regenerate the desiccant in summer. The CCHP system consisted of one engine, two heat storage tanks, and two HDCSs.

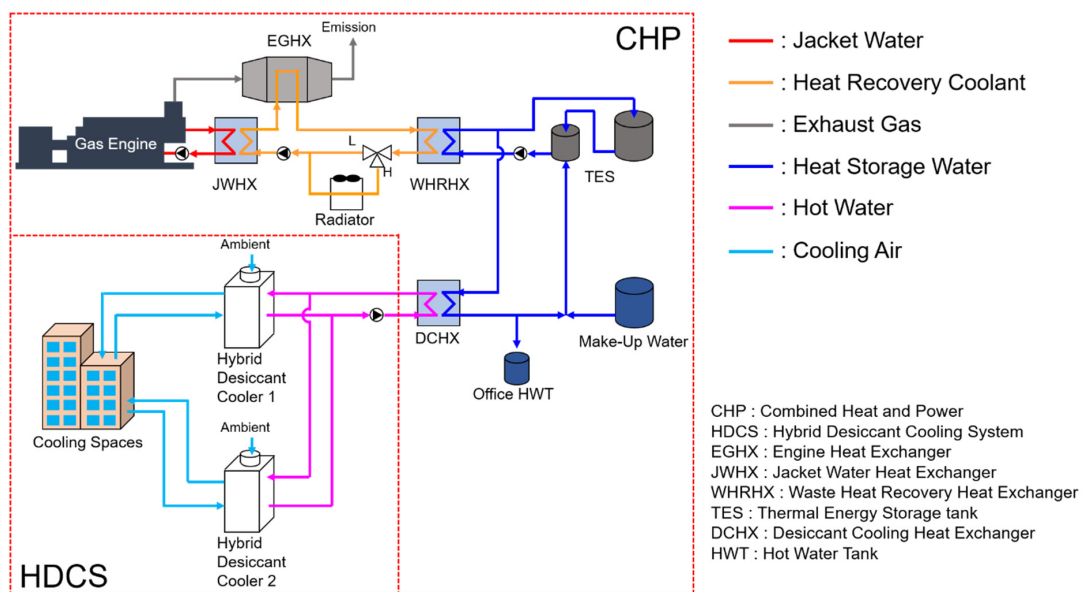


**Figure 1.** Schematic of the combined cooling, heat, and power (CCHP) system with a hybrid desiccant cooling system (HDCS).

The main specifications of this system are listed in Table 1. The maximum electric power was 115 kWe and 152 kW of waste heat was retrieved. Under the rated condition, the fuel (liquefied natural gas) consumption was 33.6 N·m<sup>3</sup>/h and the total efficiency including both electric power and heat recovery was 74.4%.

**Table 1.** Specifications of gas engine CCHP system used in the present study.

Primary Energy Input (kW)	Mechanical Power (kW)	Electric Power (kWe)	Heat Recovery (kW)	Fuel Consumption (N·m <sup>3</sup> /h)	Total Efficiency (%)
359	126	115	152	33.6	74.4

### 2.2. Hybrid Desiccant Cooling System

Figure 2a,b show a schematic and the psychrometric processes of the HDCS, respectively; 70% of the return air from the conditioned spaces (state ①) and 30% ambient air (state ⑥) are mixed to produce process air (state ②). The regeneration air of the desiccant rotor is heated by passing ambient air (state ⑥) through the condenser of the heat pump (state ⑦) and by the heat recovered from the CHP system (state ⑧) and supplied to the regeneration channel of the desiccant rotor. When the process air passes through the dehumidification channel of the desiccant rotor, the humidity decreases because of the desiccant, and the temperature increases because of the regeneration heat (processes ② and ③). Subsequently, the regeneration air is supplied to the desiccant rotor, and the moisture absorbed by the desiccant is carried over and removed (processes ⑧ and ⑨). The desiccant rotor is made of a polymeric desiccant named super desiccant polymer (SDP), whose sorption capacity is two to three times greater than that of silica gel [19]. The hot dry process air passing through the desiccant rotor is sensibly cooled as it passes through the dry channel of the regenerative evaporative cooler (REC) (processes ③ and ④). At this time, 30% of the process air is injected into the wet channel of the REC to achieve evaporative cooling. Owing to South Korea’s humid outdoor air conditions in summer, the combination of sensible heat cooling and evaporative cooling is insufficient. Therefore, in the HDCS, the process air was additionally cooled when it passed through the evaporator of the heat pump (processes ④ and ⑤).

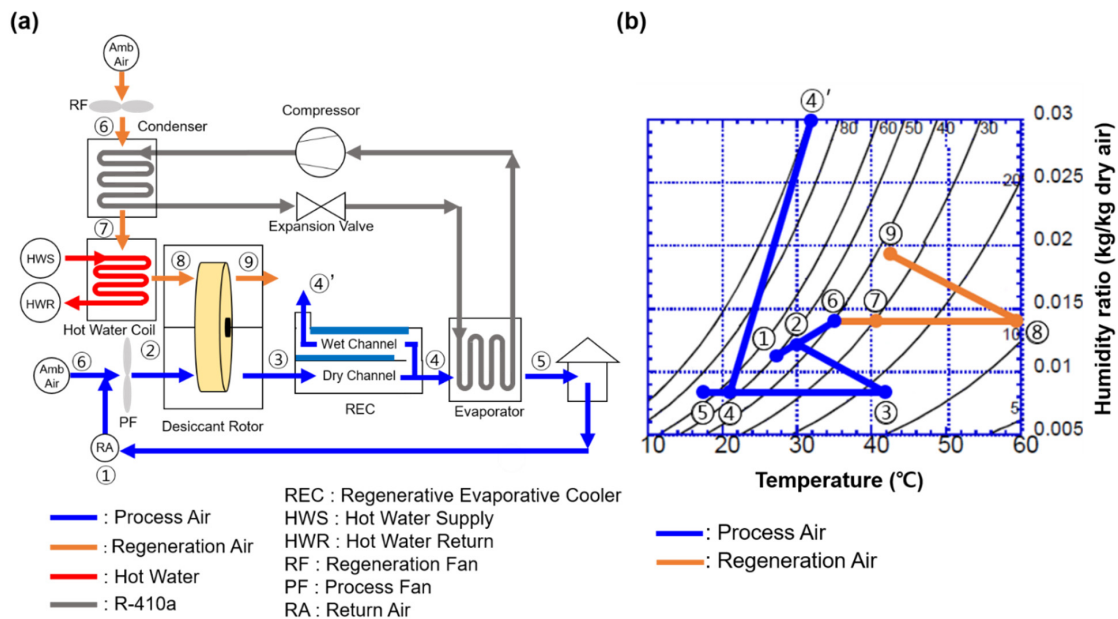


Figure 2. (a) Schematic diagram and (b) psychrometric process of an HDCS.

The specifications of the hybrid desiccant cooler are presented in Table 2. The cooling capacity of the HDCS was 9 kW and the power of the compressor driving the heat pump was 0.9 kW. The power of the process fan and return fan was 0.7 and 0.25 kW, respectively, and these values were comparable to the compressor power. The heat required to regenerate the desiccant was 6.94 kW under the design conditions.

Table 2. Specifications of HDCS.

Capacity (kW)	Compressor Power (kW)	Desiccant Rotor Power (kW)	PF Power (kW)	RF Power (kW)	Rated Regeneration Heat(kW)	$\dot{V}_P$ (m <sup>3</sup> /min)	$\dot{V}_R$ (m <sup>3</sup> /min)	Hot-Water Flow Rate (L/min)
9	0.9	0.015	0.7	0.25	6.94	23.9	20.5	8

### 2.3. Conditioned Spaces

Figure 3 shows a plan view of the conditioned spaces. There were eight supply diffusers and return ports in the three conditioned spaces. The personal office, meeting room, and part of the administration office were cooled by Unit 1 of the hybrid desiccant coolers, and Unit 2 cooled the administration office through four supply diffusers. Units 1 and 2 were identical, and their detailed specifications are presented in Table 2.

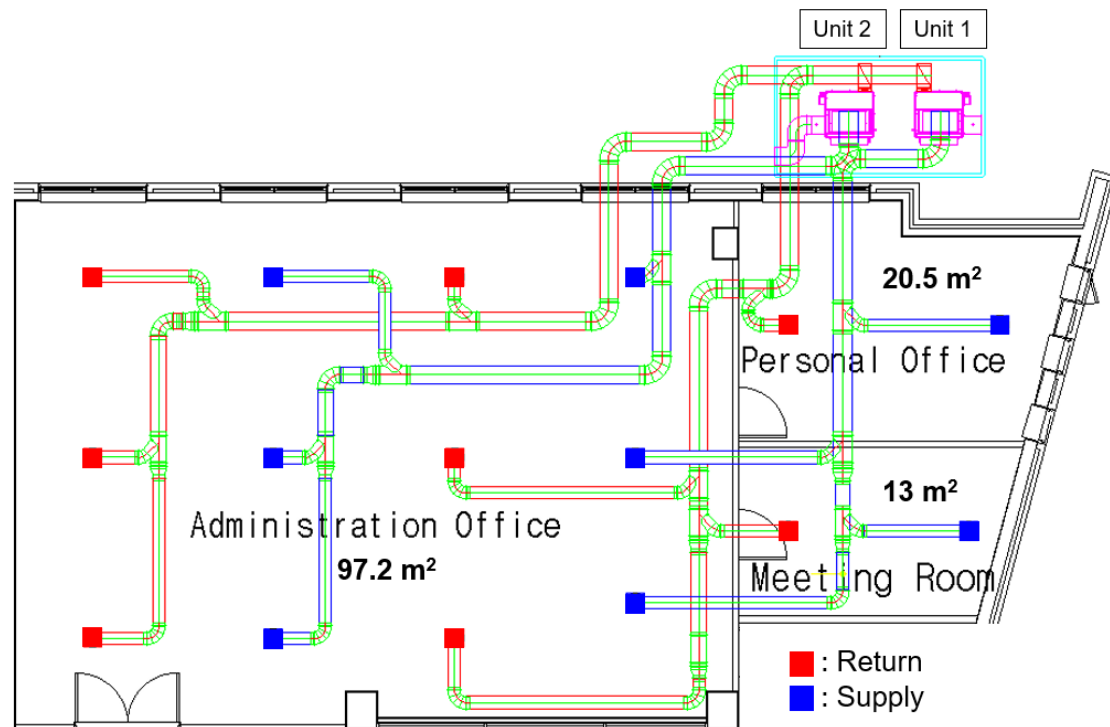


Figure 3. Floor plan of conditioned spaces with air-conditioning ducts.

## 3. Methods

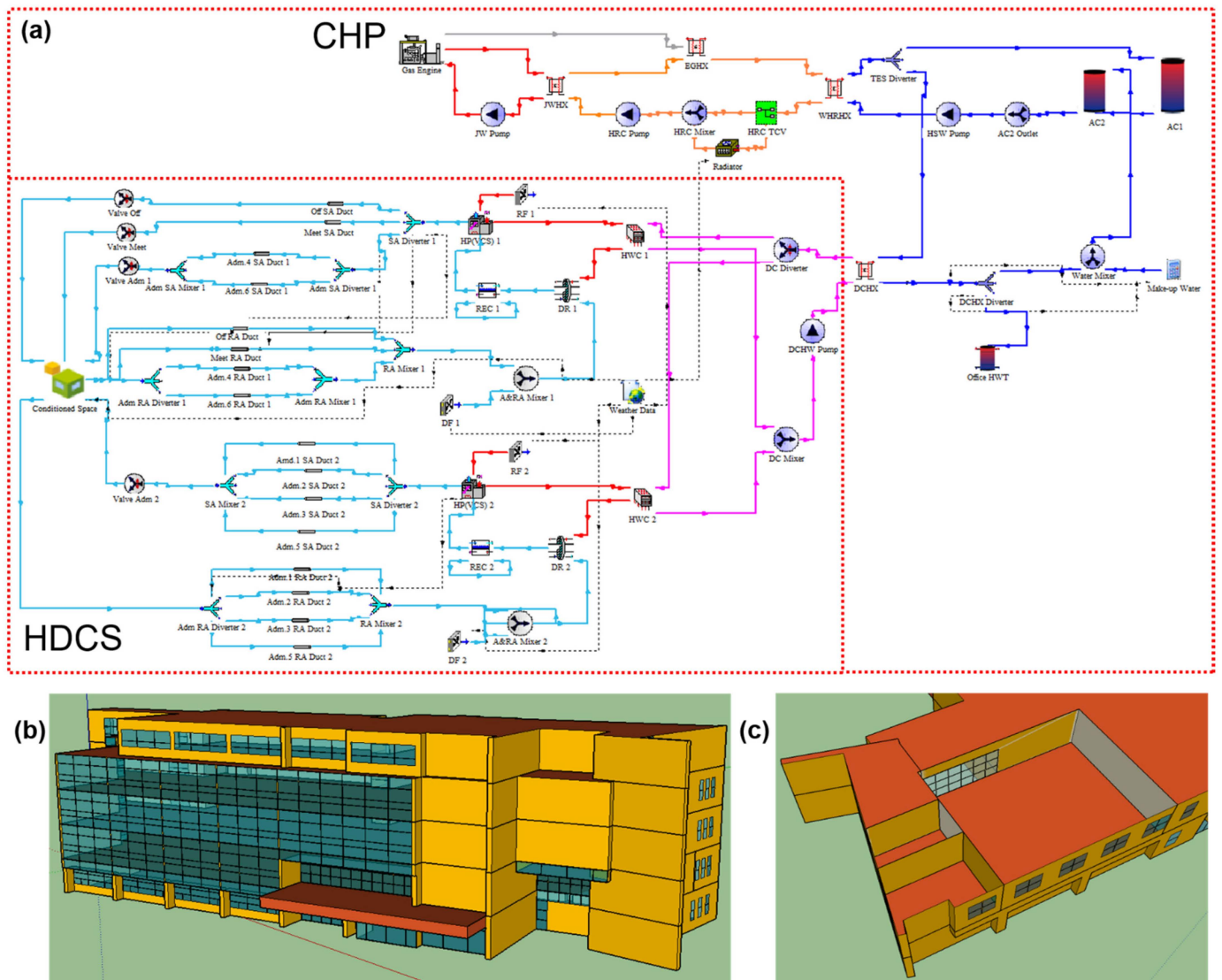
### 3.1. Simulation Models

Figure 4a shows the TRNSYS model of the system presented in Figures 1 and 2a. The gas engine, heat exchanger, heat storage tank, and heat pump constituting the system were modeled by applying their specifications to the TRNSYS component library.

The Thermal Energy System Specialists (TESS) library was used for modeling the desiccant rotor, and the target humidity and temperature were determined from the energy balance. The temperatures of the process and regeneration air were determined simultaneously from the evaporator and condenser of the heat pump.

A three-dimensional structure of the building was prepared with SketchUp (Figure 4b,c). “Conditioned Space” in Figure 4a represents the three-dimensional (3D) space in Figure 4b,c. The building shown in Figure 4 is located at 35.053227 latitude and 126.717730 longitude. It is a five-story building facing south, and the cooling space (Figures 3 and 4c) that was simulated is located on the second floor. The cooled air generated by each component in the TRNSYS simulation model of Figure 4a is supplied to the conditioned spaces of the 3D building model in Figure 4b,c, and it is subsequently returned to the TRNSYS model as the input. The simulation of the indoor conditions in the conditioned spaces was performed with TRNBuild (the TRNSYS Building Model). The dry bulb temperature and humidity ratio in each conditioned space were calculated by considering the SketchUp 3D building model in Figure 4b,c and TRNBuild [18].

Table 3 presents the indoor humidity and heat generation conditions in each space.



**Figure 4.** (a) transient system simulation tool (TRNSYS) model of the CCHP system of Figure 1, including a CHP system and an HDCS, (b) a three-dimensional (3D) office building model prepared with SketchUp, and (c) a model of conditioned spaces for TRNBuild.

**Table 3.** Indoor heat and moisture gains [20].

Type of Gain	Office			Meeting Room		
	Light	Occupancy	Device	Light	Occupancy	Device
Radiative (kJ/h·m <sup>2</sup> )	31.5	9	5	40.1	41.9	1.44
Convective (kJ/h·m <sup>2</sup> )	13.5	9	20.2	17.2	41.9	5.76
Moisture (g/h·m <sup>2</sup> )	-	7	-	-	5	-

The normal occupancy of the personal and administration offices is 1 and 9, respectively, and the meeting room is occupied only when there is a meeting. In this study, the heat generation level per unit floor area of the Swiss Society of Engineers and Architects [20] was used, and the frequent change of personnel owing to the nature of the office space was considered.

### 3.2. Governing Equations

#### 3.2.1. Desiccant Rotor

The dehumidification and regeneration characteristics of the desiccant with process air in the desiccant rotor were calculated from two potential functions, F1 and F2, and by considering the wave front propagation over the desiccant matrix proposed by Howe [21] and Jurinak [22]. Figure 5a shows the curves of F1 and F2 for silica gel; the functions are defined as

$$F1 = \frac{-2865}{T^{1.49}} + 4.344\omega^{0.8624}, \tag{1}$$

$$F2 = \frac{T^{1.49}}{6360} - 1.127\omega^{0.07969}. \tag{2}$$

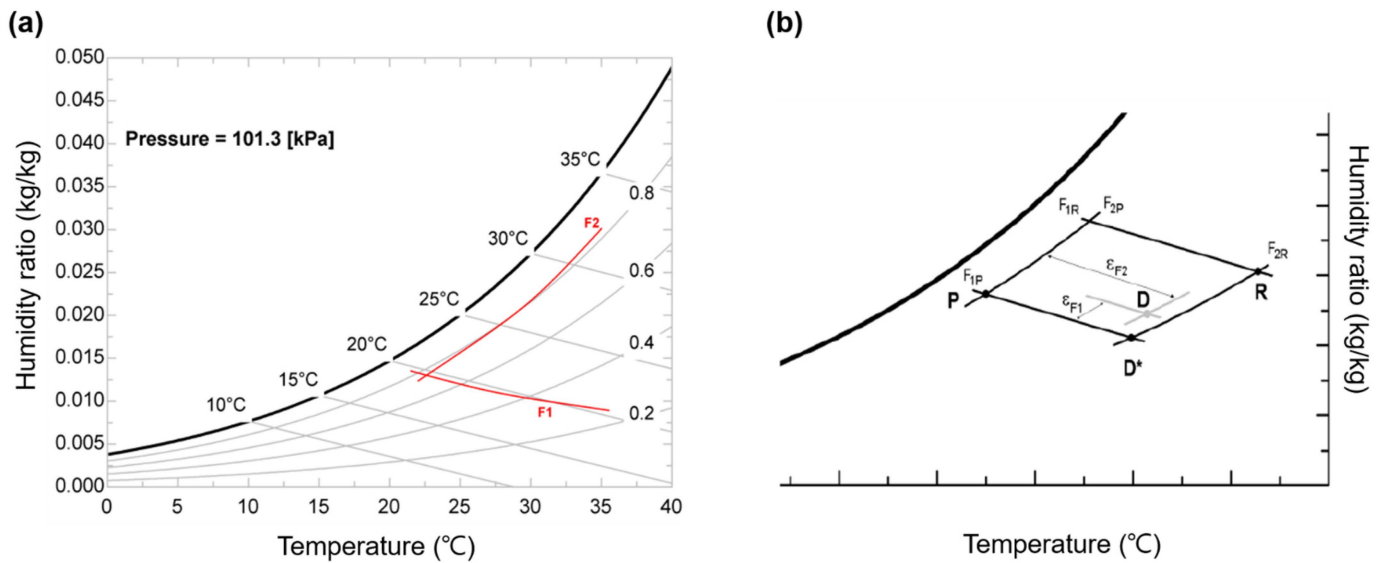


**Figure 5.** Psychrometric process of the desiccant rotor: (a) isopotential lines of F1 and F2 with wave effects [23] and (b) dehumidification and regeneration paths obtained from F1 and F2 [21].

In accordance with the two isopotential curves, F1 and F2 in Figure 5a, the process air is discharged from State P to State D\* in Figure 5b. The regeneration air becomes the state of the intersection of F1R and F2P along the F1R line from State R and is discharged to the outside. Unlike for State D\*, which is the ideal outlet state of the process air, the effectiveness [24]  $\epsilon_{F1, DR}$  and  $\epsilon_{F2, DR}$  given by Equation (3) below and proposed by Schultz were used to reflect the actual outlet state:

$$\epsilon_{Fj, DR} = \frac{Fj_{P, out} - Fj_{P, in}}{Fj_{R, in} - Fj_{P, in}} \quad (j = 1, 2). \tag{3}$$

At the design point, F1, F2,  $\epsilon_{F1, DR, design}$ , and  $\epsilon_{F2, DR, design}$  were determined using the inlet values of the dehumidification and regeneration channels of the desiccant rotor in Figure 2a. Moreover, F1 and F2 at the outlet were derived by considering the design effectiveness, F1 and F2 at the inlet, and Equation (3). Equations (1) and (2) determine the actual outlet conditions of the process air (point D in Figure 5b).

#### 3.2.2. Regenerative Evaporative Cooler

Evaporative cooling of the REC was determined from the effectiveness data validated and used in a previous study [16]. The effectiveness of REC can be defined as

$$\epsilon_{REC} = \frac{T_{DC, in} - T_{DC, out}}{T_{DC, in} - WBT_{WC, in}}. \tag{4}$$

In this case, the wet bulb temperature at the inlet of the wet channel was identical to that at the outlet of the dry channel because the working fluid passing through the wet channel was extracted from the primary air at the outlet of the dry channel with a portion of 30%.

### 3.2.3. Conditioned Spaces

For the determination of the temperatures in the conditioned spaces, the convective gains from the surfaces ( $q_{Surf}$ ), infiltration gains ( $q_{Inf}$ ), solar radiation entering the spaces through windows ( $q_{Solar}$ ), absorbed solar radiation on internal shading devices in the spaces ( $q_{ISD}$ ), indoor gains ( $q_{Gain}$ , listed in Table 3), and cooling by hybrid desiccant cooling ( $q_{Cool}$ ) should be considered (Equation (5)). For moisture balance, the mass balance in the spaces associated with infiltration and supply air was considered (Equations (6)–(8)):

$$\rho_S c_{p,s} V_S \frac{dT_S}{dt} = q_{Surf} + q_{Inf} + q_{Solar} + q_{ISD} + q_{Gain} - q_{Cool}, \quad (5)$$

$$q_{Inf} = \dot{m}_{Inf} c_{p,air} (T_{Amb} - T_S), \quad (6)$$

$$q_{Cool} = \dot{m}_{SA} c_{p,air} (T_{SA} - T_S), \quad (7)$$

$$m_S \frac{d\omega_S}{dt} = \dot{m}_{Inf} (\omega_{Amb} - \omega_S) + \dot{m}_{SA} (\omega_{SA} - \omega_S). \quad (8)$$

### 3.3. Simulation Settings and Conditions

The performance of the HDCS was simulated using KR-Kwangju-471560 weather data provided by Meteonorm (v. 5.0.013) [25]. As shown in Figure 6, 39 weather data points were extracted and used as outdoor condition scenarios. The initial temperature and humidity ratios of the conditioned spaces were the initial values of the applied ambient data. Each simulation took 6 h (from 11 a.m. to 17 p.m.). The humidity ratios of the conditioned spaces were fixed to maintain an average level of 10 g/kg three hours after the commencement of the operation, to meet the thermal comfort conditions. Furthermore, the compressor power of the heat pump and additional cooling performance of the evaporator were constant.

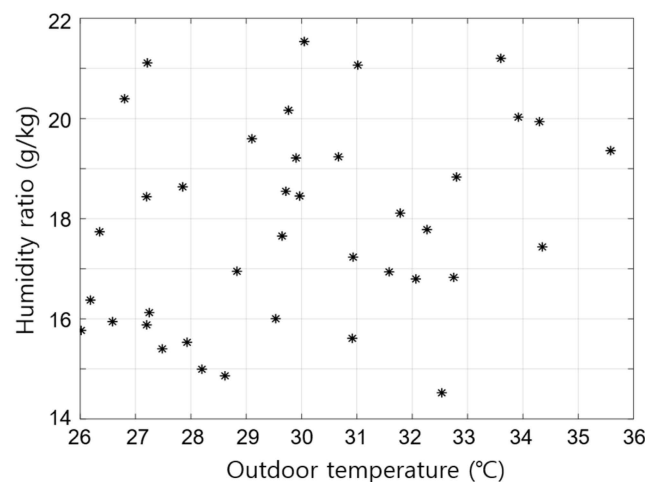


Figure 6. Outdoor conditions considered in the simulation.

## 4. Results and Discussion

### 4.1. Validation of Simulation Models

For the simulation validation, the thermal environment of the meeting room (see Figure 3) predicted by TRNSYS was compared with that observed in the experiment. The outdoor conditions and the indoor thermal environment were measured with a temperature



and humidity sensor (Testo 610), and the measurement accuracy was within 0.5 °C for the temperature and 2.5% for the relative humidity.

The ambient conditions used for the validation of the simulation models are shown in Figure 7a. In the simulation, outside air conditions similar to those of the experiments conducted for 4 h from 13:00 to 17:00 on 9 July 2019, were considered for comparing the operation results. In addition, the target temperature was set to 27 °C.

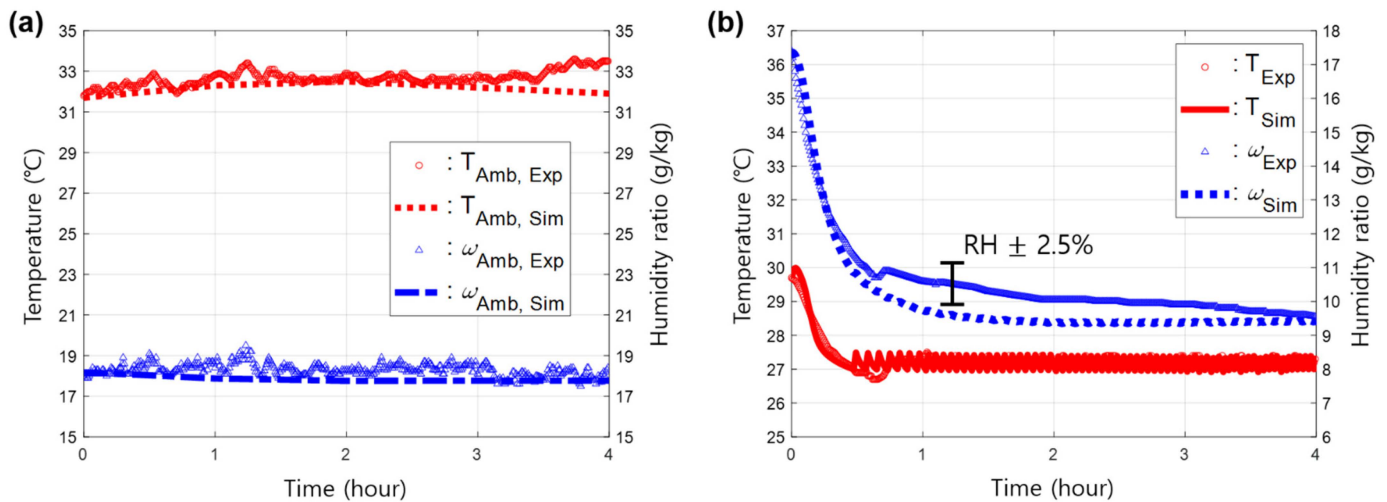


**Figure 7.** Validation of simulation model: (a) outdoor conditions and (b) temporal variation of the temperature and humidity in the meeting room.

Figure 7b compares experimental and simulated changes in the indoor thermal characteristics of the meeting room after the operation of the HDCS. Both scenarios enter the steady-state operation mode through a transient section of approximately 30 min. The steady-state temperature was accurately predicted (within 0.3 °C).

As shown in Figure 7b, it takes about 30 min to reach the steady state after start-up. The simulation reproduced the changes in the indoor thermal environment from the initial conditions to the steady state very well. At all moments within the initial 30-min transient interval, the difference between the experiment and the simulation is within the measurement error range for both temperature and humidity.

In the steady state, the temperature was predicted well within the measurement error (0.5 °C) by the simulation (compare the red symbol and line in Figure 7b), but the humidity was underpredicted by the simulation in the initial steady-state region. The maximum error occurred a little over 1 h after the simulation start-up, and the measured humidity ratio of 10.5 g/kg was predicted as 9.6 g/kg. When driving for 4 h, the humidity ratio obtained in the simulation converged to the same value as in the experiment. The TRNSYS simulation results for the indoor thermal environment (presented later) were extracted from the results of operation for 6 h from start-up.

#### 4.2. Thermal Comfort

Figure 8 presents a comparison of the thermal comfort conditions of each space obtained in the simulations under ambient conditions for 39 days (Figure 6), with experimental data obtained with an actual system. The experimental data (yellow dots) show that the indoor thermal environment did not meet the thermal comfort conditions in some of the 39 outdoor condition scenarios. According to the simulation results, because the desiccant capacity was increased to maintain an indoor humidity ratio of 10 g/kg regardless of the outdoor humidity level, all cooling spaces met the thermal comfort conditions. In the simulation, the humidity and indoor temperature decreased because the space was evaporatively cooled with process air with a humidity ratio of approximately 9.5 g/kg.

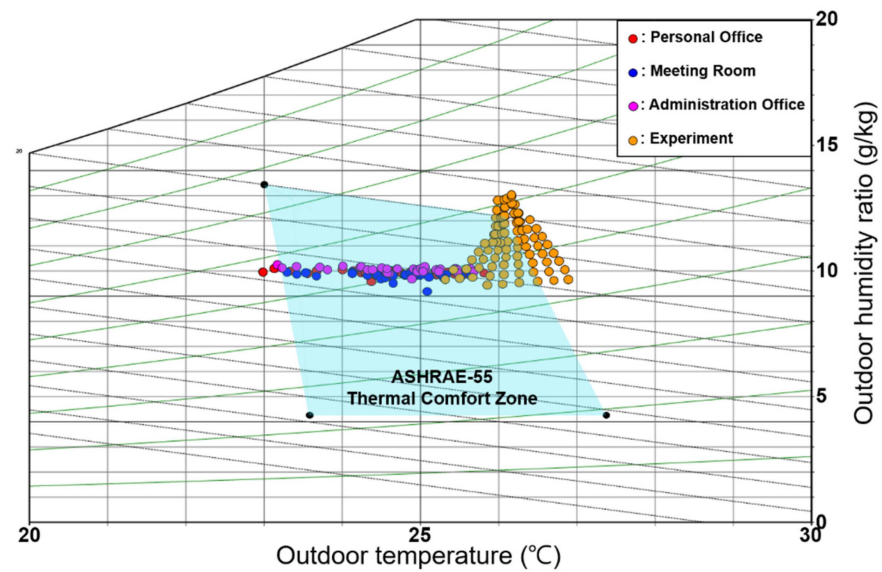


**Figure 8.** Changes in thermal comfort conditions of cooling spaces with an increase in the desiccant rotor capacity.

#### 4.3. Regeneration Heat and Cooling Capacity

A definition of regeneration heat is provided in Equation (9). Regeneration heat is heat rate to heat up the regeneration air by hot water produced by CHP.

$$q_{Reg} = \dot{m}_R(h_{HWC, out} - h_{HWC, in}). \tag{9}$$

Figure 9a,b show the regeneration heat required to maintain the humidity ratio of each space at an average of 10 g/kg during 3–6 h operation according to the ambient conditions. Similar to the results of the regeneration heat obtained from the field tests in the residential environment in Figure 9c, more regeneration heat is required under low temperature and high humidity conditions in this case. The desiccant rotor used in the field test had a limited dehumidification capacity, and therefore, compensating for the increasing outdoor humidity ratio was difficult. Consequently, the regeneration heat demand remained at approximately 3 kW under humid conditions. However, in the simulation, the capacity of the desiccant rotor was increased, and the prediction results indicated the use of up to 6.14 kW of regeneration heat. Furthermore, regenerative heat was not required since the heat from the condenser of the heat pump was sufficient to maintain an indoor humidity ratio of 10 g/kg under low humidity conditions.

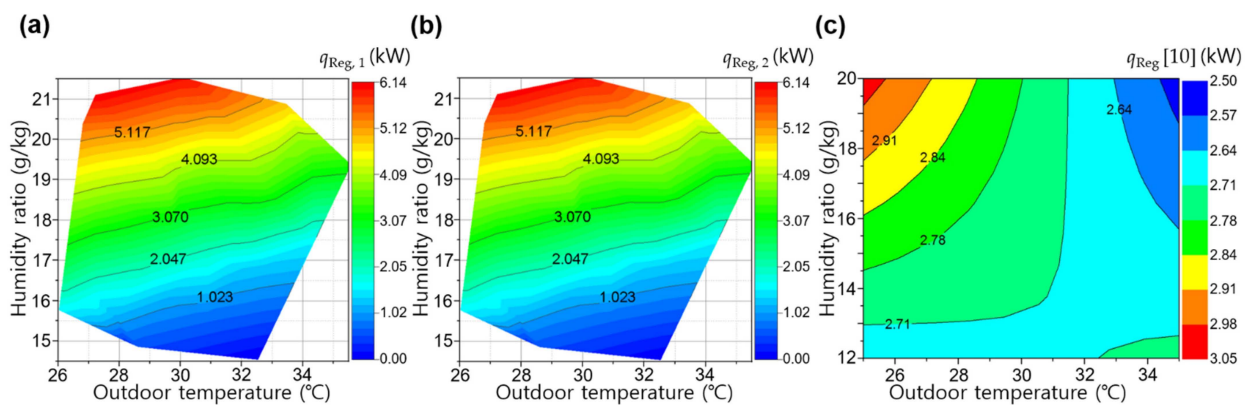


**Figure 9.** Regeneration heat of (a) Unit 1 and (b) Unit 2. (c) Field test data [10] of regeneration heat for the existing system.

Figure 10a,b present the simulated cooling capacities (Equation (7)) with respect to the ambient conditions. To maintain an indoor humidity ratio of 10 g/kg in the simulation, the higher the humidity level, the more the amount of latent heat that is treated, and the cooling capacity increases. According to the prediction results, after dehumidification with the desiccant rotor, evaporative cooling with the REC improves with increasing outdoor temperature. Accordingly, the cooling capacity is high under high temperature and humidity conditions. However, the results of the field test (Figure 10c) show that the cooling capacity increases under low temperature and high humidity conditions. As the desiccant rotor of the HDCS used in the field test had limited capacity, it was impossible to dehumidify the supply air (approximately 9.5 g/kg humidity remained). Furthermore, cooling the space sufficiently with evaporative cooling only was difficult at the high humidity level, and therefore, dependence on the heat pump increased. Consequently, the cooling capacity was high at low outdoor temperatures.

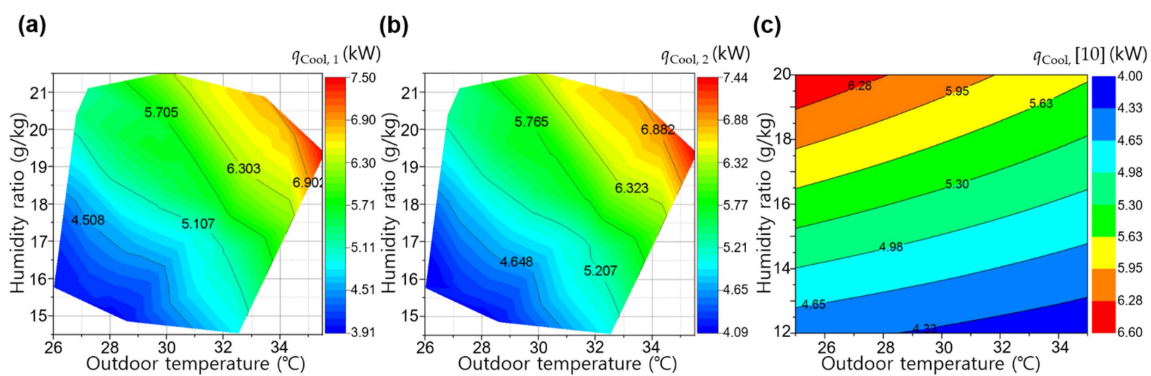


Figure 10. Cooling capacity of (a) Unit 1 and (b) Unit 2. (c) Field test data [10] of cooling capacity for the existing system.

#### 4.4. Coefficient of Performance

Equation (10) defines the COP and Figure 11a,b show the simulation results for the COP, based on Equation (10). Less regeneration heat is required under hot and dry conditions (Figure 9a,b), and the cooling capacity is high under hot and humid conditions (Figure 10a,b). In the 39 simulated scenarios, the regeneration heat ranges from 0 to 6.14 kW, and the cooling capacity ranges from approximately 4 to 7.5 kW. The COP is high under hot and dry conditions since regeneration heat is more sensitive to ambient conditions. In the actual system, the cooling capacity was more sensitive to the outdoor air conditions than to regeneration heat (see Figures 9c and 10c). Therefore, the COP tended to behave in a similar manner to the cooling capacity: it was high under low temperature and high humidity conditions (see Figure 11c).

$$COP = \frac{q_{Cool}}{q_{Reg} + W_{Elc}} \tag{10}$$

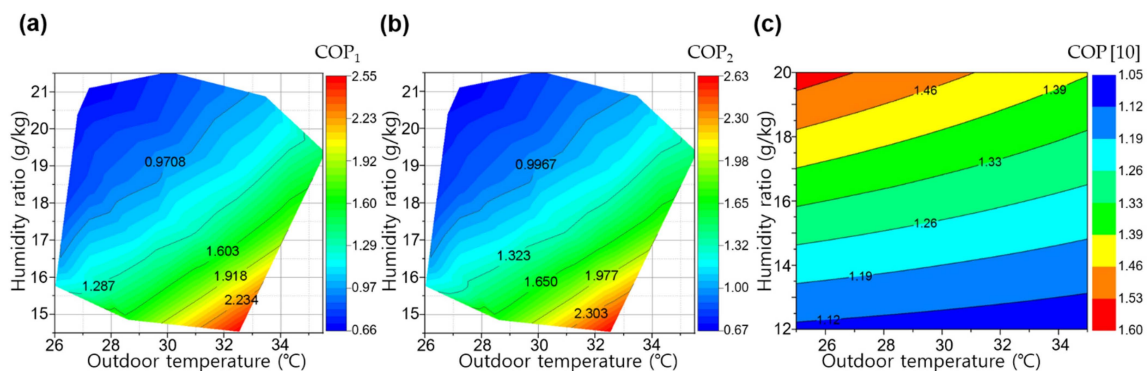
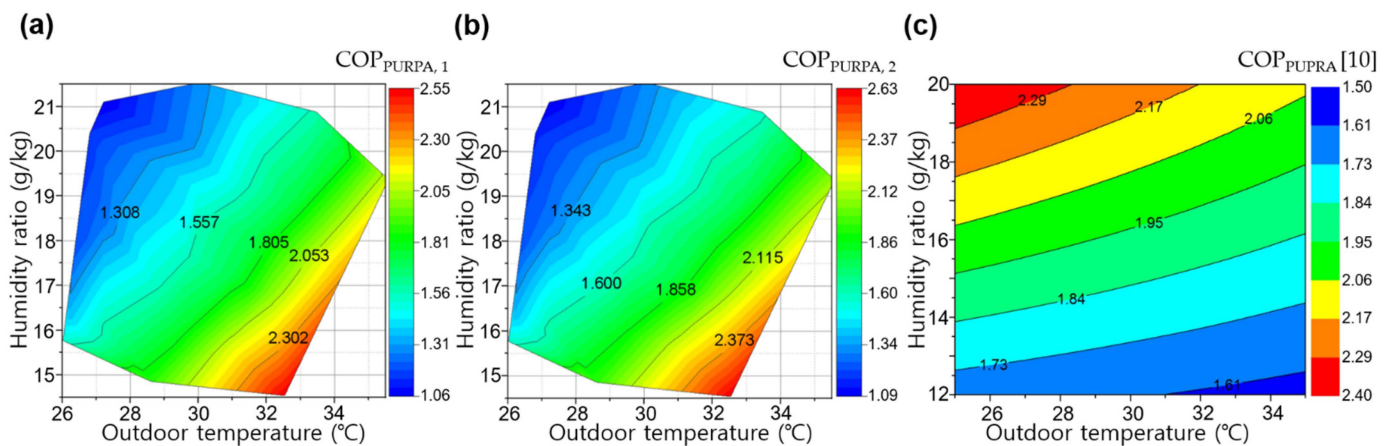


Figure 11. Coefficient of performance (COP) for (a) Unit 1 and (b) Unit 2. (c) Field test data [10] of the COP of the existing system.

In the calculation of the COP of the HDCS, which used the exhaust heat of the gas engine, the COP was determined by correcting the values of the driving energy sources, heat and electricity. A definition of the COP reflecting a heat-to-electricity ratio of 1:2 as provided in the Public Utility Regulatory Policies Act (PURPA) is provided in Equation (11) below [26].

$$\text{COP}_{\text{PURPA}} = \frac{q_{\text{Cool}}}{0.5q_{\text{Reg}} + W_{\text{Elc}}} \quad (11)$$

Even if the heat value is recalculated (Figure 12a,b), the trend of the COP does not change significantly with respect to the ambient conditions. While the overall distribution is similar to those in Figure 11a,b, the slopes of the contours in Figure 12a,b are steeper because of the reduced influence of the regeneration heat, which is sensitive to the outdoor humidity ratio. As the level of regenerative heat is considered half that of electricity,  $\text{COP}_{\text{PURPA}}$  has a larger value compared with the COP under identical ambient conditions. The change in the distribution according to the COP definition in the actual system is similar (Figures 11c and 12c).



**Figure 12.** COP with thermoelectric value ( $\text{COP}_{\text{PURPA}}$ ) from the Public Utility Regulatory Policies Act (PURPA) for (a) Unit 1 and (b) Unit 2. (c) Field test data [10] of the COP for the existing system.

## 5. Conclusions

In this paper, the performance change with the capacity of the desiccant rotor in an HDCS linked to a cogeneration system was predicted with TRNSYS. The capacity of the desiccant rotor was increased to reduce the humidity ratio of the process air to 9.5 g/kg, and subsequently, the thermal comfort conditions of the cooling space were evaluated. Furthermore, the cooling capacity, regeneration heat, and COP were predicted and compared with data from an actual system. The main conclusions are as follows.

1. When the capacity of the desiccant rotor was increased, the amount of used regeneration heat with respect to the outside air conditions increased 1.7 times. According to this result and the simulations, the thermal environment of the cooling space entered the ASHRAE comfort zone even under outdoor conditions that were outside the thermal comfort zone of the actual system.
2. When the capacity of the desiccant rotor was increased, the simulated cooling capacity improved compared with the cooling capacity of the actual system by 10%. Actual systems have high cooling capacities under low temperature and high humidity conditions. A simulation was conducted to investigate the effect of an increase in the dehumidification capacity on the cooling capacity under hot and humid conditions.
3. Increasing the capacity of the desiccant rotor rendered the COP more sensitive to temperature compared with the COPs of conventional systems. The existing system had a high COP under low temperature and high humidity conditions. However, when the dehumidification capacity increased, the COP was high under high temper-

ature and dry conditions. These characteristics are similar to those of a pure desiccant cooling system.

4. Less regeneration heat was required in hot and dry outdoor conditions. While the cooling capacity increased in hot and humid conditions. The variation of the regeneration heat ranged from 0 to 6.14 kW, while the cooling capacity varied from 3.91 to 7.5 kW. Accordingly, if the capacity of the desiccant rotor was sufficient to match the humidity ratio of the process air to 9.5 g/kg, then the COP was determined by the regeneration heat rather than the cooling capacity.
5. In the HDCS, when the capacity of the desiccant rotor was increased to an extent where the humidity ratio of the process air could be reduced to 9.5 g/kg, the simulated overall efficiency of the CHP could be increased while ensuring suitable thermal comfort conditions in the cooling spaces.

**Author Contributions:** Simulations, J.H.K.; analysis, J.A. and J.H.K.; writing, J.A. and J.H.K.; supervision, J.A. All authors have read and agreed to the published version of the manuscript.

**Funding:** This research study was supported by the Korea Electric Power Corporation (grant number: R18XA06-36).

**Institutional Review Board Statement:** Not applicable.

**Informed Consent Statement:** Not applicable.

**Data Availability Statement:** Data is contained within this article.

**Conflicts of Interest:** The authors declare no conflict of interest.

## Nomenclature

ASHRAE	American Society of Heating, Refrigerating, and Air-Conditioning Engineers
CCHP	combined cooling, heat, and power
CHP	combined heat and power
COP	coefficient of performance
COP <sub>PURPA</sub>	coefficient of performance reevaluated in PURPA
$c_{p, air}$	specific heat of air (kJ/kg·K)
DCHX	desiccant cooling heat exchanger
EDT	effective draft temperature
EGHX	exhaust gas heat exchanger
F1	isopotential function 1 for dehumidification with silica gel
F2	isopotential function 2 for dehumidification with silica gel
HDCS	hybrid desiccant cooling system
HWC	hot-water coil
HWR	hot-water return
HWS	hot-water supply
HWT	hot-water tank
$h$	enthalpy (kJ/kg)
JWHX	jacket water heat exchanger
$m$	mass (kg)
$\dot{m}$	mass flow rate (kg/s)
PF	process fan
PMV	predicted mean vote
$p$	property
$q_{Cool}$	cooling capacity (kW)
$q_{Gain}$	indoor gains resulting from occupancy, devices, and light (kW)
$q_{Inf}$	infiltration gains (kW)
$q_{ISD}$	absorbed solar radiation on internal shading devices in the spaces (kW)
$q_{Reg}$	regeneration heat (kW)

$q_{Surf}$	convective gains from the surfaces (kW)
$q_{Solar}$	solar radiation entering the spaces through windows (kW)
RA	return air
REC	regenerative evaporative cooler
RF	regeneration fan
RH	relative humidity (%)
T	dry bulb temperature (°C)
SAP	super absorbent polymer
SDP	super desiccant polymer
TES	thermal energy storage tank
TESS	thermal energy system specialists
$t$	time (s or h)
$V$	volume (m <sup>3</sup> )
$\dot{V}$	volume flow rate (m <sup>3</sup> /min)
WBT	wet bulb temperature (°C)
WHRHX	waste heat recovery heat exchanger
$W_{Elec}$	electric power (kW)
<b>Greek Letters</b>	
$\rho$	density (kg/m <sup>3</sup> )
$\epsilon$	effectiveness
$\epsilon$	relative error (%)
$\omega$	humidity ratio (g/kg of dry air)
<b>Subscripts</b>	
Amb	ambient
Design	design value
DC	dry channel of REC
DR	desiccant rotor
Exp	experiment
Inf	infiltration
in	inlet
out	outlet
P	process air
R	regeneration air
S	space
SA	supply air
Sim	simulation
WC	wet channel of REC
1	Unit 1 of hybrid desiccant coolers
2	Unit 2 of hybrid desiccant coolers

## References

1. Badami, M.; Portoraro, A. Performance analysis of an innovative small-scale trigeneration plant with liquid desiccant cooling system. *Energy Build.* **2009**, *41*, 1195–1204. [\[CrossRef\]](#)
2. Angrisani, G.; Minichiello, F.; Roselli, C.; Sasso, M. Desiccant HVAC system driven by a micro-CHP: Experimental analysis. *Energy Build.* **2010**, *42*, 2028–2035. [\[CrossRef\]](#)
3. Sahlot, M.; Riffat, S.B. Desiccant cooling systems: A review. *Int. J. Low Carbon Tech.* **2016**, *11*, 489–505. [\[CrossRef\]](#)
4. Sultan, M.; El-Sharkawy, I.I.; Miyazaki, T.; Saha, B.B.; Koyama, S. An overview of solid desiccant dehumidification and air conditioning systems. *Renew. Sustain. Energy Rev.* **2015**, *46*, 16–29. [\[CrossRef\]](#)
5. Vivekh, P.; Kumja, M.; Bui, D.T.; Chua, K.J. Recent developments in solid desiccant coated heat exchangers—A review. *Appl. Energy* **2018**, *229*, 778–803. [\[CrossRef\]](#)
6. Seo, J.N.; Kim, Y.I.; Chung, K.S. Dynamic simulation of a hybrid desiccant cooling utilizing heat pump, desiccant and evaporative cooler. *Trans. Korea Soc. Geotherm. Energy Eng.* **2011**, *7*, 45–50.
7. Khalid, A.; Mahmood, M.; Asif, M.; Muneer, T. Solar assisted, pre-cooled hybrid desiccant cooling system for Pakistan. *Renew. Energy* **2008**, *34*, 151–157. [\[CrossRef\]](#)
8. Pi, C.-H.; Kang, B.H.; Chang, Y.S. Performance analysis of a desiccant rotor for rotational period in a desiccant cooling system. *Trans. Korean Soc. Mech. Eng. B* **2012**, *36*, 523–531. [\[CrossRef\]](#)
9. Hwang, W.-B.; Choi, S.; Lee, D.-Y. In-depth analysis of the performance of hybrid desiccant cooling system incorporated with an electric heat pump. *Energy* **2017**, *118*, 324–332. [\[CrossRef\]](#)

10. Ahn, J.; Kim, J.; Kang, B.H. Performance of a hybrid desiccant cooling system in a residential environment. *Heat Transf. Eng.* **2016**, *37*, 633–639. [[CrossRef](#)]
11. Ahn, J.; Choi, H.Y. Effects of supply angle on thermal environment of residential space with hybrid desiccant cooling system for multi-room control. *Appl. Sci.* **2020**, *10*, 7271. [[CrossRef](#)]
12. Enescu, D. A review of thermal comfort models and indicators for indoor environments. *Renew. Sustain. Energy Rev.* **2017**, *79*, 1353–1379. [[CrossRef](#)]
13. Kim, J.; Ahn, J. Heat transfer characteristics of heat storage tank driven by gas engine cogeneration system. *Korean J. Air Cond. Refrig. Eng.* **2019**, *31*, 322–331.
14. Jani, D.B.; Mishra, M.; Sahoo, P.K. Performance analysis of a solid desiccant assisted hybrid space cooling system using TRNSYS. *J. Build. Eng.* **2018**, *19*, 26–35. [[CrossRef](#)]
15. Caliskan, H.; Hong, H.; Jang, J.K. Thermodynamic assessments of the novel cascade air cooling system including solar heating and desiccant cooling units. *Energy Convers. Manag.* **2019**, *199*, 112013. [[CrossRef](#)]
16. Jani, D.B.; Bhabhor, K.; Dadi, M.; Doshi, S.; Jotaniya, P.V.; Ravat, H.; Bhatt, K. A review on use of TRNSYS as simulation tool in performance prediction of desiccant cooling cycle. *J. Therm. Anal. Calorim.* **2020**, *140*, 2011–2031. [[CrossRef](#)]
17. Sudhakar, K.; Jenkins, M.S.; Mangal, S.; Priya, S.S. Modeling of a solar desiccant cooling system using a TRNSYS-MATLAB co-simulator: A review. *J. Build. Eng.* **2019**, *24*, 100749. [[CrossRef](#)]
18. Kim, J.; Ahn, J. Simulation of multi-room controlled desiccant cooling system considering the structure of the cooling space. *Korean J. Air Cond. Refrig. Eng.* **2020**, *32*, 263–271.
19. Lee, J.; Lee, D.Y. Sorption characteristics of a novel polymeric desiccant. *Int. J. Refrig.* **2012**, *35*, 1940–1949. [[CrossRef](#)]
20. Swiss Society of Engineers and Architects. *SIA 2024*; Swiss Society of Engineers and Architects: Zurich, Switzerland, 2015.
21. Howe, R.R. Model and Performance Characteristics of a Commercially-Sized Hybrid Air Conditioning System which Utilizes a Rotary Desiccant Dehumidifier. Master's Thesis, University of Wisconsin—Madison, Madison, WI, USA, 1983.
22. Jurinak, J.J. Open Cycle Solid Desiccant Cooling: Component Models and System Simulations. Ph.D. Thesis, University of Wisconsin—Madison, Madison, WI, USA, 1982.
23. Solar Energy Lab. *TRNSYS, Version 18*; Software for Transient System Simulation; Solar Energy Lab: Madison, WI, USA, 2018.
24. Schultz, K.J. The Performance of Desiccant Dehumidifier Air-Conditioning Systems Using Cooled Dehumidifiers. Master's Thesis, University of Wisconsin—Madison, Madison, WI, USA, 1983.
25. *Meteonorm: KR-Kwangju-471560*; Meteotest: Bern, Switzerland, 1995.
26. Federal Energy Regulatory Commission. *Public Utility Regulatory Policies Act of 1978*; Federal Energy Regulatory Commission: Washington, DC, USA, 1978.